Jurnal Ilmiah Berkala: Sains dan Terapan Kimia
Vol.20 No. 2, July 2026

In Silico Identification of Natural Compounds as Potential FGF2 Inhibitors for Glioblastoma Therapy

Identifikasi Senyawa Alami Secara In Silico sebagai Inhibitor FGF2 Potensial untuk Terapi Glioblastoma

Nico Berlinson Fernando[1], Siti Hodijah[1] Agus Kartono[1], and Setyanto Tri Wahyudi[1]*

[1]Department of Physics, Faculty of Mathematics and Natural Sciences, IPB University, Bogor, 16680, Indonesia

**Email: stwahyudi@apps.ipb.ac.id*

ABSTRACT

Glioblastoma multiforme (GBM) is the most aggressive primary malignant brain tumor and remains difficult to treat due to its high level of invasion, resistance to therapy, and poor prognosis. Fibroblast growth factor 2 (FGF2) plays a crucial role in glioblastoma development by increasing glioma cell proliferation, angiogenesis, and the maintenance of glioblastoma cancer stem cells. Therefore, this study aims to identify candidate FGF2 inhibitors from natural compounds through virtual screening and molecular docking approaches. The binding sites on FGF2 were identified through protein-protein docking approaches between FGF2 and FGFR1-FGFR4, then used as the basis for virtual screening of 1,496 natural compounds using AutoDock Vina. Compounds that showed competitive binding energy were further analyzed using targeted and blind docking with AutoDock4. The results showed that Pyranoamentoflavone, 5,3',5'-Trihydroxy-6,7,4'-trimethoxyflavone, Sotetsuflavone, and Isotrilobine have competitive binding affinity to the active site of FGF2. These findings indicate that these four compounds have potential as FGF2 inhibitor candidates for the development of targeted therapies for GBM. However, further validation through molecular dynamics simulations as well as in vitro and in vivo studies is still needed to confirm their binding stability, safety, and therapeutic efficacy.

Keywords: *GBM; FGF2; natural compounds; molecular docking; virtual screening*

Received: 21 April 2026; **Accepted**: 15 July 2026; **Available online**: 29 July 2026

1. INTRODUCTION

Glioblastoma (GBM) is a type of malignant brain tumor classified as a grade IV tumor by the World Health Organization (WHO) classification. GBM has a poor prognosis, with a median survival of only 12–15 months despite standard therapy (Lee et al., 2018).

One of the main reasons for the low therapeutic success is the presence of a subpopulation of stem cell-like cells (CSCs) that are resistant to cytotoxic therapy. Furthermore, the high rate of genomic mutations in GBM further increases therapy resistance and enhances treatment strategies

(Garnier et al., 2019). Various therapeutic strategies have been implemented in the treatment of GBM, including surgical resection, radiotherapy, and chemotherapy based on alkylating agents such as temozolomide (TMZ) and antiangiogenic agents such as bevacizumab. However, these therapeutic advances have not significantly improved the prognosis of GBM patients in recent decades (Kumari & Kumar, 2023).

Epidemiologically, the annual incidence of primary malignant brain tumors is reported to reach 7.08 cases per 100,000 population (Ostrom et al., 2020). Therefore, the development of more effective targeted therapies remains a major focus of research to improve the therapeutic efficacy and prognosis of GBM patients. Fibroblast Growth Factor 2 (FGF2) is an oncogenic factor that plays a crucial role in the development of glioblastoma (GBM), primarily through its ability to increase glioma cell proliferation, stimulate angiogenesis, and maintain self-renewal properties in glioblastoma cancer stem cells (GBM CSCs) (Haley & Kim, 2014; Toyoda et al., 2013). Based on these roles, the FGF2/FGFR signaling pathway is a promising therapeutic target for inhibiting GBM progression.

Experimental evidence suggests that FGF2 inhibition using antisense oligonucleotides and specific antibodies effectively suppresses glioma cell proliferation and angiogenesis (Haley & Kim, 2014). In addition to FGF2, this pathway can also be targeted at the FGFR receptor level. FGFR1 is the most studied receptor because it is associated with poor prognosis, increased glioma cell migration, GSC maintenance, and increased tumorigenicity in vivo. Conversely, FGFR1 inhibition suppresses tumor growth and GSC migration (Kowalski-Chauvel et al. 2019; Jimenez-Pascual et al. 2019).

Unlike FGFR1, the roles of FGFR2, FGFR3, and FGFR4 in GBM remain incompletely understood. FGFR2 is associated with the regulation of glioma progression, FGFR3 is known to undergo oncogenic fusion (FGFR3-TACC3) in some glioma cases, while FGFR4 has low expression levels and its biological function in GBM is still unclear (Di Stefano et al., 2015; Jimenez-pascual et al., 2019). Thus, targeting FGF2 is considered more potential than targeting a single FGFR receptor because FGF2 acts as an upstream regulator that initiates the activation of all members of the FGFR family (FGFR1–FGFR4) (Ornitz & Itoh, 2015). Research on the use of natural compounds as glioblastoma therapy candidates has continued to grow in recent decades because these compounds possess various pharmacological activities, including antitumor, antioxidant, antiviral, and anti-inflammatory activities (Copolovici et al., 2017).

One approach widely used in the early stages of drug discovery is virtual screening through molecular docking, which is able to predict the binding affinity and orientation of ligands to target proteins at the atomic level (Kiametis et al., 2017). This approach is widely used in the drug discovery process because it can accelerate the selection of candidate compounds more efficiently in terms of time and cost (Meng et al., 2011).

Among the various molecular docking software packages available, AutoDock Vina and AutoDock4 are two widely used software packages because they are able to predict binding poses with the lowest binding energy in a relatively short computation time (Chen et al., 2023; Trott & Olson, 2010). Therefore, this study aims to identify glioblastoma therapy candidates derived from natural compounds through virtual screening and molecular docking approaches.

2. MATERIALS AND METHODS

2.1. Materials

The crystal structure of Fibroblast Growth Factor 2 (FGF2; PDB ID: 4OEE) and the crystal structures of fibroblast growth factor receptors including FGFR1 (PDB ID: 5EW8), FGFR2 (PDB ID: 3B2T), FGFR3 (PDB ID: 6PNX), and FGFR4 (PDB ID: 4QQT) were obtained from the Protein Data Bank (PDB) (https://www.rcsb.org/). A total of 1,496 natural compounds were collected from several scientific articles and the UI Herbal database. The structures of these compounds were then downloaded from the PubChem database in SDF format.

2.2. Method

2.2.1 Selection of FGF2 target protein structures

A total of 22 crystal structures of FGF2 (homo sapiens) are available in the UniProt database (P09038). Target protein structures were selected based on X-ray imaging, resolution ≤ 2.5 Å, 100% sequence identity, and annotation as FGF2.

Based on these criteria, the FGF2 structure with PDB ID 4OEE was selected as the target protein due to its 100% sequence identity and the highest resolution (1.50 Å). The three-dimensional structure of the protein was downloaded from the Protein Data Bank (PDB) (https://www.rcsb.org/). Next, the FGF2 protein structure was separated from water molecules and attached substrate using VMD.

2.2.2 Prediction of FGF2 binding sites

Identification of FGF2 binding sites was carried out by utilizing its natural interactions with the crystal structures of the FGFR1 (PDB ID: 5EW8), FGFR2 (PDB ID: 3B2T), FGFR3 (PDB ID: 6PNX), and FGFR4 (PDB ID: 4QQT) receptors. Binding site prediction was performed using the ZDOCK 3.0.2 server (https://zdock.umassmed.edu/) through the protein–protein docking method. The docking results were analyzed to identify FGF2 residues that interact with each receptor. These residues were then used as a reference in determining the binding site and grid box position in the molecular docking process.

2.2.3 Ligand preparation

In this study, a total of 1,496 active compounds were compiled from several scientific articles and the UI Herbal Database (HerbalDB), a database of Indonesian medicinal plant compounds developed by the University of Indonesia and still publicly accessible at the time of dataset collection. The chemical structures of the active compounds were downloaded from PubChem (https://pubchem.ncbi.nlm.nih.gov/) in SDF format.

Next, the ligand structures were geometrically optimized using ORCA. The optimized structures were first converted to PDB format using Open Babel and then further converted to PDBQT format using AutoDockTools 1.5.7 (Forli et al., 2016) for use in the molecular docking process.

2.2.4 Virtual screening using AutoDock Vina

Virtual screening of 1,496 natural compounds was performed through molecular docking analysis using AutoDock Vina at four previously identified FGF2 binding sites. The entire docking process was performed using the same parameters for each binding site. The docking results were then sorted based on the obtained binding energy values.

The five compounds with the most negative binding energy values at each binding site were selected as initial candidates for further analysis. From these candidates, compounds identified at more than one binding site were further evaluated based on

drug-likeness and validated through targeted docking and blind docking using AutoDock4.

2.2.5 Drug-likeness prediction

Compounds identified at more than one binding site were then evaluated using SwissADME (http://www.swissadme.ch/) (Daina et al., 2017) to predict physicochemical, pharmacokinetic, and drug-likeness characteristics. Drug-likeness evaluation was performed based on Lipinski's Rule of Five, which includes a molecular mass <500 g/mol, hydrogen bond donor (HBD) ≤ 5, hydrogen bond acceptor (HBA) ≤ 10, logP value ≤ 5, and molar refractivity in the range of 40–130 (Mustafa et al., 2020).

In addition, Pan-Assay Interference Structures (PAINS) analysis was performed to identify molecular substructures that could potentially cause interference in various bioassays, resulting in false positives. This analysis is used as an initial screening stage to minimize the selection of compounds with non-specific biological activity (Baell & Holloway, 2010).

2.2.6 Further analysis of selected compounds using AutoDock4

In targeted docking, the docking process was performed using the Lamarckian Genetic Algorithm (LGA) with 25,000,000 energy evaluations, a population size of 300, and 100 iterations (runs). The resulting docking poses were then clustered using an RMSD tolerance of 2.0 Å. For each compound, the pose with the lowest binding energy value from the dominant cluster was selected as a representation of the docking results. The interactions between the ligand and amino acid residues in the FGF2 protein were then analyzed and visualized using LigPlot+. Next, blind docking was performed using the same parameters as targeted docking, but with an expanded search space to cover the entire surface of the FGF2 protein. At this stage, three grid spacing variations were used, namely 0.375 Å, 0.500 Å, and 0.625 Å, to evaluate the effect of grid resolution on the docking results.

3. RESULTS AND DISCUSSION

3.1. Identification of FGF2 binding sites

Identification of FGF2 binding sites was performed through protein-protein docking with FGFR1, FGFR2, FGFR3, and FGFR4. **Table 1** presents a visualization of the interaction sites between FGF2 and FGFR1, FGFR2, FGFR3, and FGFR4, along with the FGF2 amino acid residues involved in these interactions. The protein-protein docking results indicate that FGF2 interacts with FGFR1, FGFR2, FGFR3, and FGFR4 through different amino acid residues on the protein surface.

In binding site 1, the residues involved include Arg97, Arg109, Thr112, Lys110, Trp114, and Gln134. Binding site 2 consists of Tyr24, Phe31, Lys46, Ser100, Gly133, and Leu140, while binding site 3 involves Pro14, Tyr24, Glu59, Gly61, Leu98, and Asr102. Binding site 4 is composed of Lys26, Phe31, Arg42, Glu45, Pro49, Arg120, Lys135, and Met142. Differences in the residues involved in each binding site indicate that FGF2 has multiple interface areas that can interact with members of the FGFR family. These residues were then used as references in determining binding sites for molecular docking of test compounds with the FGF2 protein.

Table 1 Interaction sites of FGF2 with FGFR1–FGFR4 predicted by protein–protein docking

Binding Site	Binding Area	FGF2 Amino Acid Residues
1	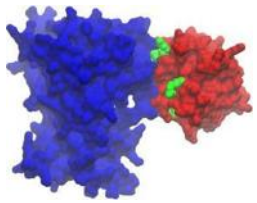	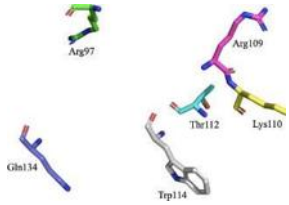
2	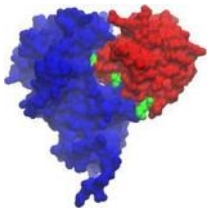	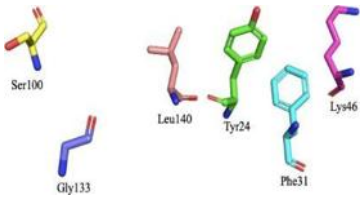
3	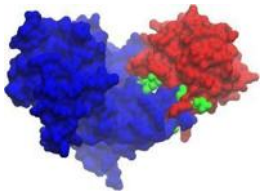	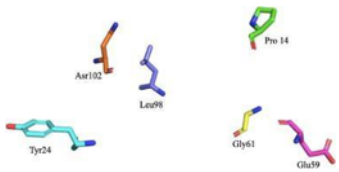
4	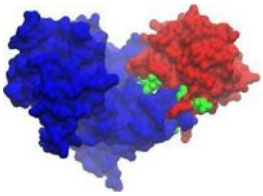	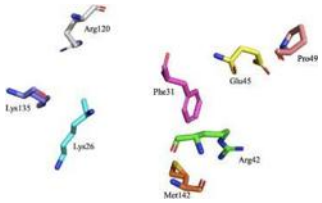

Note: Red indicates FGF2, blue indicates FGFR, and green indicates the protein–protein interaction interface.

3.2. Virtual screening of compounds against FGF2

Molecular docking is a computational method widely used in drug discovery and design to predict the binding mode of ligands to target proteins. This method allows for the evaluation of binding affinity based on binding energy and identifies interaction patterns between ligands and residues in the protein's active site (Sivakumar et al., 2020).

In this study, molecular docking of 1,496 natural compounds was performed using AutoDock Vina at four previously identified FGF2 binding sites. **Fig. 1** shows the distribution of binding energy values resulting from molecular docking of 1,496 natural compounds at each FGF2 binding site. All compounds are sorted based on their binding energy values, with candidates with the highest binding affinity at the beginning of the graph. This distribution indicates that only a small proportion of compounds have competitive binding affinity for the target protein. Based on the distribution of binding energy values, the five compounds with the most negative binding energy values at each binding site were selected as initial candidates and presented in **Table 2**. The more negative the binding energy value obtained, the stronger the interaction between the ligand and the target protein (Khan et al., 2025). Based on **Table 2**, pyranoamentoflavone is included in

the five best candidates and appears at all binding sites while 5,3',5'-trihydroxy-6,7,4'-trimethoxyflavone appears at binding sites 1, 2, and 4. Isotrilobine appears at binding sites 1 and 4, and sotetsuflavone at binding sites 1 and 2. The consistency of the appearance of the four compounds at several binding sites indicates a competitive binding affinity to FGF2 so they were selected as candidates for further analysis using AutoDock4.

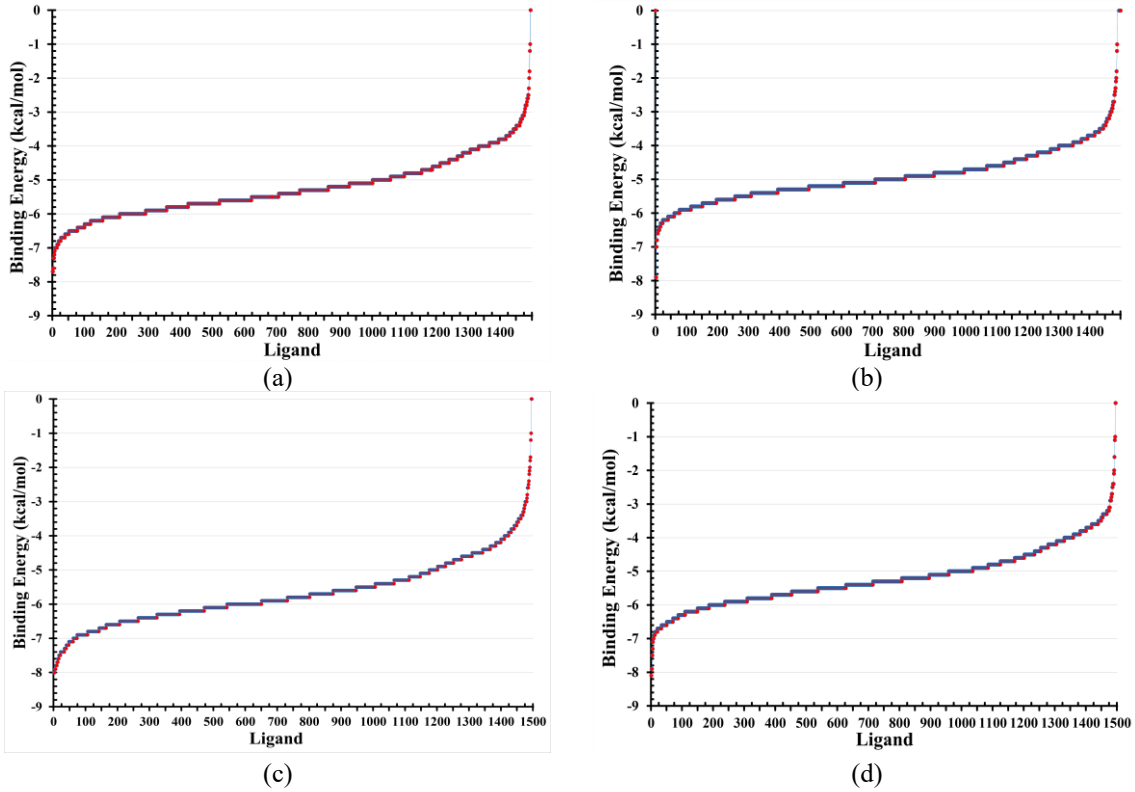

Figure 1. Distribution of binding energy values for 1,496 natural compounds at the four FGF2 binding sites obtained from molecular docking using AutoDock Vina: (a) binding site 1, (b) binding site 2, (c) binding site 3, and (d) binding site 4

Table 2 Top five compounds with the most negative binding energies at each FGF2 binding site

Binding Site FGF2	Information	CID	Compound	Binding Energy (kcal/mol)
1	Top 1	21581557	5,3',5'-Trihydroxy-6,7,4'-trimethoxyflavone	-7.7
	Top 2	21582613	Pyranoamentoflavone	-7.7
	Top 3	12310578	Isotrilobine	-7.6
	Top 4	442728	Cassiamin C	-7.3
	Top 5	5494868	Sotetsuflavone	-7.3

Binding Site FGF2	Information	CID	Compound	Binding Energy (kcal/mol)
2	Top 1	21581557	5,3',5'-Trihydroxy-6,7,4'-trimethoxyflavone	-7.9
	Top 2	21582613	Pyranoamentoflavone	-7.9
	Top 3	5280486	Raucaffricine	-7.0
	Top 4	441876	Agavoside A	-6.8
	Top 5	5494868	Sotetsuflavone	-6.8
3	Top 1	5322012	Grossamide	-8.0
	Top 2	12302850	Chandalone	-8.0
	Top 3	5281246	Mutatochrome	-7.9
	Top 4	21582613	Pyranoamentoflavone	-7.9
	Top 5	102034490	(4*aR*,4*bS*,7*S*,8*aS*,10*aS*)-3-[2-[(2*R*,4*aS*,4*bS*,8*aS*)-2,4*b*,8,8-tetramethyl-4,4*a*,5,6,7,8*a*,9,10-octahydro-3*H*-phenanthren-2-yl]-2-oxoethyl]-7-ethenyl-4*b*,7,10*a*-trimethyl-1-methylidene-5,6,8,8*a*,9,10-hexahydro-4*aH*-phenanthren-2-one	-7.9
4	Top 1	5281694	Robustaflavone	-8.1
	Top 2	21581557	5,3',5'-Trihydroxy-6,7,4'-trimethoxyflavone	-7.9
	Top 3	21582613	Pyranoamentoflavone	-7.9
	Top 4	12310578	Isotrilobine	-7.5
	Top 5	42607760	6,4'-Dihydroxyaurone 4-O-rutinoside	-7.3

3.3. Drug-likeness properties of selected compounds

Lipinski's Rule of Five (Ro5) is used as an initial parameter to predict the potential of a compound as a drug candidate with good oral bioavailability based on its structural characteristics. A compound that meets all rules or has only one violation can still be considered as a potential drug candidate (Mustafa et al., 2022). The analysis results presented in **Table 3** show that 5,3',5'-trihydroxy-6,7,4'-trimethoxyflavone does not violate Lipinski's rule, while pyranoamentoflavone and sotetsuflavone each show one violation. Meanwhile, isotrilobine shows two violations of Lipinski's rule. Nevertheless, these results still provide an initial picture that most compounds have structural characteristics that still support their potential as oral drug candidates. In addition to Ro5, PAINS analysis was used to evaluate the possibility of molecular structures that can cause false-positive results in biological tests. All compounds showed 0 PAINS structural alerts, indicating that no structural fragments were found that could potentially interfere with the results of biological tests (Abdizadeh, 2024). Based on pharmacokinetic predictions, 5,3',5'-trihydroxy-6,7,4'–trimethoxyflavone and isotrilobine have high GI absorption, so they are predicted to have better oral absorption potential than

pyranoamentoflavone and sotetsuflavone. In addition, most of the compounds are predicted not to be P-glycoprotein (P-gp) substrates, so they have the potential to not experience efflux mediated by this transporter. Overall, the results of this evaluation indicate that all four compounds have their respective advantages and limitations. However, the absence of PAINS alerts and the presence of pharmacokinetic parameters that still support these compounds indicate that these compounds remain relevant to be considered in further studies as FGF2 inhibitor candidates.

Table 3. Physicochemical parameters and predicted pharmacokinetic profiles of the selected compounds

Compound	Pyranoamentoflavone	5,3',5'-Trihydroxy-6,7,4' -trimethoxyflavone	Isotrilobine	Sotetsuflavone
Molecular weight (g/mol)	604.56	360.31	576.68	552.48
No of rotatable bonds	3	4	2	4
Num. H-bond acceptor	10	8	7	10
Num. H-bond donor	5	3	0	5
TPSA (Å^2)	170.8	118.59	52.63	170.8
Lipinski rule of 5	1	0	2	1
PAINS alerts	0	0	0	0
Pgp substrate	No	Yes	No	No
GI absorption	Low	High	High	Low

3.4. Advanced analysis of selected compounds using targeted docking AutoDock4

Based on the results of virtual screening using AutoDock Vina, four compounds with competitive binding affinities were selected for further analysis using targeted docking with AutoDock4. The use of different search algorithms and scoring functions in AutoDock4 is expected to provide a more comprehensive evaluation and increase confidence in the docking results (Chen et al., 2023). The results of targeted docking using AutoDock4 for the four selected compounds at each FGF2 binding site are presented in **Tables 4** and **5**. Based on the data in **Table 4**, pyranoamentoflavone showed the best binding affinity compared to other compounds with the most negative binding energy value of -7.90 kcal/mol at binding site 2. In addition, this compound was the only compound identified at all binding sites, indicating the ability to interact at various FGF2 binding areas. The compound 5,3',5'-trihydroxy-6,7,4'-trimethoxyflavone also showed relatively good binding affinity, especially at binding site 4, with a binding energy of -7.03 kcal/mol. Meanwhile, isotrilobine showed the best binding affinity at binding site 1, with a binding energy of -6.88 kcal/mol, while sotetsuflavone showed lower binding affinity than the other compounds. The positions of the compounds resulting from targeted docking on the surface of the FGF2 protein are shown in **Fig. 2**.

The reliability of the targeted docking results was further evaluated based on the entropy parameters and the percentage of cluster conformation, as presented in **Table 5**.

Isotrilobine showed the highest percentage of cluster conformation, at 100% at binding sites 1 and 4, with an entropy value of 0.00. These results indicate that all the resulting docking poses are concentrated in a single dominant cluster, indicating high reproducibility of the binding mode. Pyranoamentoflavone has a cluster percentage ranging from 36–64%, while 5,3',5'-trihydroxy-6,7,4'-trimethoxyflavone has a cluster percentage ranging from 31–48%. On the other hand, sotetsuflavone exhibits a relatively lower cluster percentage (33–35%), indicating that the docked conformation is more variable than the other compounds. This finding supports the reliability of the docking poses, which were subsequently used for residue interaction analysis in the FGF2 protein.

Table 4 Binding energy values from targeted docking of selected compounds against FGF2

Compound	Local/ Indonesian Name	Scientific Name	Binding site 1	Binding site 2	Binding site 3	Binding site 4
Pyranoamentoflavone	Nyamplung	*Calophyllum Inophyllum)*	-6.01	-7.9	-6.00	-7.04
5,3',5'-Trihydroxy-6,7,4' - trimethoxyflavone	Kemuning	*Murraya Paniculata*	-5.93	-5.13	-	-7.03
Isotrilobine	Cincau minyak	*Stephania Hernandifolia*	-6.88	-	-	-5.50
Sotetsuflavone	Jambe	*Cycas Revoluta*	-4.88	-4.75	-	-

Note: The "-" sign indicates that docking was not performed because the compound was not selected at the relevant binding site based on the virtual screening results using AutoDock Vina.

Table 5 Conformational cluster analysis of selected compounds based on targeted docking results

Binding site	Compound	Entropy	Conformation cluster (%)
1	5,3',5'-Trihydroxy-6,7,4' trimetoxyflavone	0.23	46
	Pyranoamentoflavone	0.17	64
	Isotrilobine	0.00	100
	Sotetsuflavone	0.45	35
2	5,3',5'-Trihydroxy-6,7,4'-trimethoxyflavone	0.32	48
	Pyranoamentoflavone	0.37	36
	Sotetsuflavone	0.45	33
3	Pyranoamentoflavone	0.34	51
4	5,3',5'-Trihydroxy-6,7,4'-trimethoxyflavone	0.43	31
	Pyranoamentoflavone	0.43	36
	Isotrilobine	0.00	100

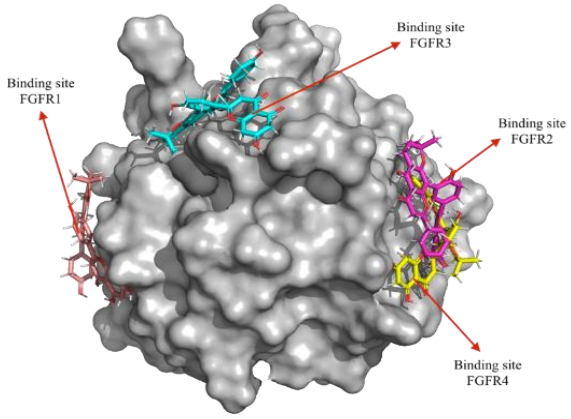

Figure 2. Binding pose of selected compounds resulting from targeted docking on the FGF2 protein

The pose with the lowest binding energy, derived from the dominant cluster, was then selected as a representative for further interaction analysis using LigPlot+ (**Fig. 3**). Pyranoamentoflavone and 5,3',5'-trihydroxy-6,7,4'-trimethoxyflavone showed similar interaction patterns by forming three hydrogen bonds with residues Arg44, Lys135, and Tyr103, as well as a number of hydrophobic interactions with residues Arg120, Gly28, Lys26, Phe31, Met142, Lys46, Leu140, and Tyr24.

In contrast to these two compounds, isotrilobine did not form hydrogen bonds and only interacted through hydrophobic contacts with residues Glu78, Lys110, Ser113, Thr112, Trp114, and Tyr111. Meanwhile, sotetsuflavone formed two hydrogen bonds with Thr112 as well as hydrophobic interactions with Glu78, Arg109, Lys110, Tyr111 and Trp114.

3.5. Blind docking analysis of selected compounds using AutoDock 4.2.6

After targeted docking at the predetermined binding sites, the four selected compounds were then analyzed using blind docking with AutoDock 4.2.6. Unlike targeted docking, which focuses on a specific binding site, this approach allows identification of the pose with the lowest binding energy without any binding site restrictions. The blind docking results are presented in **Table 6**, while the best pose on the FGF2 protein surface is visualized in **Fig. 4**.

All compounds yielded negative binding energy values at all three grid spacing variations (0.375, 0.500, and 0.625 Å), indicating that all compounds were still able to interact with the FGF2 protein even when docked without restrictions on specific binding sites. Furthermore, changes in grid spacing did not significantly impact the binding energy values obtained, so the blind docking results were relatively consistent at each grid resolution used.

The obtained binding energy values ranged from −6.08 to −7.19 kcal/mol. Sotetsuflavone showed the most negative binding energy value of −7.19 kcal/mol at a grid spacing of 0.375 Å, while pyranoamentoflavone, 5,3',5'-trihydroxy-6,7,4'-trimethoxyflavone, and isotrilobine showed the most negative binding energy values of −6.73, −6.84, and −6.52 kcal/mol, respectively.

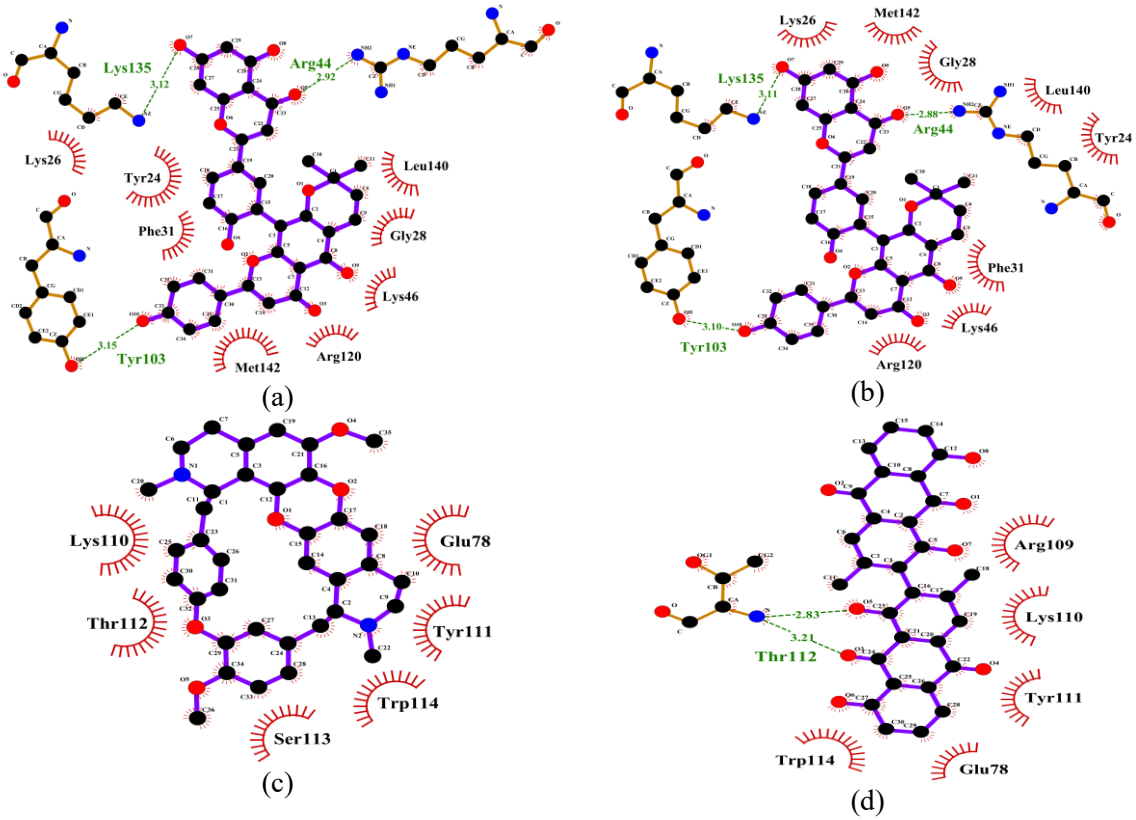

Figure 3. Interaction diagram of the best poses of selected compounds against FGF2, (a) Pyranoamentoflavone, (b) 5,3',5'-Trihydroxy-6,7,4'-trimethoxyflavone, (c) Isotrilobine, and (d) Sotetsuflavone

Table 6 Binding energy values from blind docking of selected compounds with FGF2

Compound	Grid spacing (Å)		
	0.375	0.500	0.625
Pyranoamentoflavone	-6.73	-6.39	-6.15
5,3',5'-Trihydroxy-6,7,4'-trimethoxyflavone	-6.15	-6.84	-6.22
Sotetsuflavone	-7.19	-6.76	-6.29
isotrilobine	-6.52	-6.29	-6.08

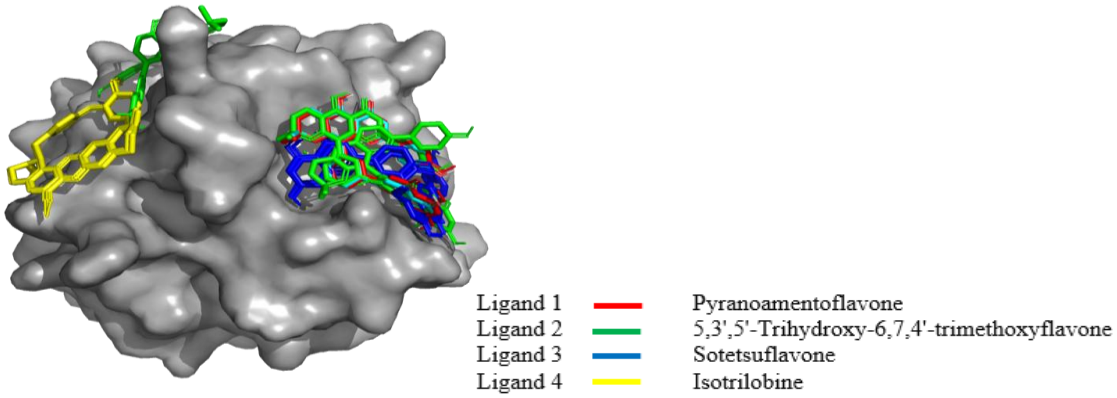

Figure 4. Binding pose of selected compounds resulting from blind docking on the FGF2 protein

4. CONCLUSIONS

In this study, four potential binding sites on the FGF2 protein identified through a protein-protein docking approach with the FGFR1-FGFR4 receptors were used as the basis for virtual screening using molecular docking of 1,496 Indonesian natural compounds. Based on the results of virtual screening using AutoDock Vina, four compounds were selected that consistently showed competitive binding energy values at several binding sites to be further validated using AutoDock4 through targeted docking and blind docking. The analysis results showed that pyranoamentoflavone, 5,3',5'-trihydroxy-6,7,4'-trimethoxyflavone, sotetsuflavone, and isotrilobine have competitive binding affinity to the FGF2 protein. Therefore, these four compounds have the potential as FGF2 inhibitor candidates and require further validation through molecular dynamics simulations as well as in vitro and in vivo studies in the development of targeted glioblastoma therapy based on FGF2 inhibition.

LIST OF REFERENCES

Abdizadeh, T. (2024). Identification of novel potential inhibitors of monkeypox virus thymidine kinase using molecular docking, molecular dynamics simulation and MM/PBSA methods. *Molecular Diversity*, *28*(4), 2513–2546. https://doi.org/10.1007/s11030-023-10692-w

Baell, J. B., & Holloway, G. A. (2010). New substructure filters for removal of pan assay interference compounds (PAINS) from screening libraries and for their exclusion in bioassays. *Journal of Medicinal Chemistry*, *53*(7), 2719–2740. https://doi.org/10.1021/jm901137j

Chen, T., Shu, X., Zhou, H., Beckford, F. A., & Misir, M. (2023). Algorithm selection for protein–ligand docking: strategies and analysis on ACE. *Scientific Reports*, *13*(1), 1–15. https://doi.org/10.1038/s41598-023-35132-5

Copolovici, D., Bungau, S., Boscencu, R., Tit, D. M., & Copolovici, L. (2017). The fatty acids composition and antioxidant activity of walnut cold press oil. *Revista de Chimie*, *68*(3), 507–509.

Daina, A., Michielin, O., & Zoete, V. (2017). SwissADME: a free web tool to evaluate pharmacokinetics, drug-likeness and medicinal chemistry friendliness of small molecules. *Scientific Reports*, *7*(1), 42717. https://doi.org/10.1038/srep42717

Di Stefano, A. L., Fucci, A., Frattini, V., Labussiere, M., Mokhtari, K., Zoppoli, P., Marie, Y., Bruno, A., Boisselier, B., Giry, M., Savatovsky, J., Touat, M., Belaid, H., Kamoun, A., Idbaih, A., Houillier, C., Luo, F. R., Soria, J.-C., Tabernero, J., … Lavarone, A. (2015). Detection, characterization, and inhibition of FGFR–TACC fusions in IDH wild-type glioma. *Clinical Cancer Research*, *21*(14), 3307–3317. https://doi.org/10.1158/1078-0432.CCR-14-2199

Forli, S., Huey, R., Pique, M. E., Sanner, M. F., Goodsell, D. S., & Olson, A. J. (2016). Computational protein–ligand docking and virtual drug screening with the AutoDock suite. *Nature Protocols*, *11*(5), 905–919. https://doi.org/10.1038/pj.2016.37

Garnier, D., Renoult, O., Alves-Guerra, M. C., Paris, F., & Pecqueur, C. (2019). Glioblastoma Stem- Like Cells , Metabolic Strategy to Kill a Challenging Target. *Frontiers in Oncology*, *9*(118), 1–18. https://doi.org/10.3389/fonc.2019.00118

Haley, E. M., & Kim, Y. (2014). The role of basic fibroblast growth factor in glioblastoma multiforme and glioblastoma stem cells and in their in vitro culture. *Cancer Letters*, *346*(1), 1–5.

https://doi.org/10.1016/j.canlet.2013.12.003

Jimenez-pascual, A., Hale, J. S., Kordowski, A., Pugh, J., Silver, D. J., Bayik, D., Roversi, G., Alban, T. J., Rao, S., Chen, R., Mcintyre, T. M., Colombo, G., Taraboletti, G., Holmberg, K. O., Forsberg-nilsson, K., Lathia, J. D., & Siebzehnrubl, F. A. (2019). ADAMDEC1 maintains a growth factor signaling loop in cancer stem cells. *Cancer Discovery*, *9*(11), 1574–1589. https://doi.org/10.1158/2159-8290.CD-18-1308

Khan, W. M. A., Alam, M. J., Sherwani, S., Alouffi, S., Al-Motair, K., Khan, S., & Khan, S. N. (2025). Molecular docking and simulation analysis of glioblastoma cell surface receptors and their ligands: identification of inhibitory drugs targeting fibronectin ligand to potentially halt glioblastoma pathogenesis. *International Journal of Molecular Sciences*, *26*(20), 10038. https://doi.org/10.3390/ijms262010038

Kiametis, A. S., Silva, M. A., Romeiro, L. A., Martins, J. B., & Gargano, R. (2017). Potential acetylcholinesterase inhibitors: molecular docking, molecular dynamics, and in silico prediction. *Journal of Molecular Modeling*, *23*(2), 67. https://doi.org/10.1007/s00894-017-3228-9

Kumari, S., & Kumar, P. (2023). Design and computational analysis of an mmp9 inhibitor in hypoxia-induced glioblastoma multiforme. *ACS Omega*, *8*(11), 10565–10590. https://doi.org/10.1021/acsomega.3c00441

Lee, A. E., Yong, R. L., Paddison, P., & Zhu, J. (2018). Comparison of glioblastoma (GBM) molecular classification methods. *Seminars in Cancer Biology*, *53*, 201–211. https://doi.org/10.1016/j.semcancer.2018.07.006

Meng, X.-Y., Zhang, H.-X., Mezei, M., & Cui, M. (2011). Molecular docking: a powerful approach for structure-based drug discovery. *Current Computer-Aided Drug Design*, *7*(2), 146–157. https://doi.org/10.2174/157340911795677602

Mustafa, G., Mahrosh, H. S., Zafar, M., Attique, S. A., & Arif, R. (2022). Exploring the antihyperglycemic potential of tetrapeptides devised from AdMc1 via different receptor proteins inhibition using in silico approaches. *International Journal of Immunopathology and Pharmacology*, *36*, 1–15. https://doi.org/10.1177/03946320221103120

Mustafa, G., Majid, M., Ghaffar, A., Yameen, M., Samad, H. A., & Mahrosh, H. S. (2020). Screening and molecular docking of selected phytochemicals against NS5B polymerase of hepatitis C virus. *Pakistan Journal of Pharmaceutical Sciences*, *33*(5), 2317–2322. https://doi.org/10.36721/PJPS.2020.33.5.SUP.2317-2322.1

Ornitz, D. M., & Itoh, N. (2015). The fibroblast growth factor signaling pathway. *Wiley Interdisciplinary Reviews: Developmental Biology*, *4*(3), 215–266. https://doi.org/10.1002/wdev.176

Ostrom, Q. T., Patil, N., Cioffi, G., Waite, K., Kruchko, C., & Barnholtz-sloan, J. S. (2020). CBTRUS statistical report: primary brain and other central nervous system tumors diagnosed in the United States in 2013–2017. *Neuro-Oncology*, *22*(1), iv1–iv96. https://doi.org/10.1093/neuonc/noaa200

Sivakumar, K. C., Haixiao, J., Naman, C. B., & Sajeevan, T. P. (2020). Prospects of multitarget drug designing strategies by linking molecular docking and molecular dynamics to explore the protein–ligand recognition process. *Drug Development Research*, *81*(6), 685–699.

https://doi.org/10.1002/ddr.21673

Toyoda, K., Tanaka, K., Nakagawa, S., Thuy, D. H. D., Ujifuku, K., Kamada, K., Hayashi, K., Matsuo, T., Nagata, I., & Niwa, M. (2013). Initial contact of glioblastoma cells with existing normal brain endothelial cells strengthen the barrier function via fibroblast growth factor 2 secretion: a new in vitro blood–brain barrier model. *Cellular and Molecular Neurobiology*, *33*(4), 489–501. https://doi.org/10.1007/s10571-013-9913-z

Trott, O., & Olson, A. J. (2010). AutoDock Vina: improving the speed and accuracy of docking with a new scoring function, efficient optimization, and multithreading. *Journal of Computational Chemistry*, *31*(2), 455–461. https://doi.org/10.1002/jcc.21334